

Search for Neutral Higgs Bosons Decaying to Tau Pairs in $p\bar{p}$ Collisions at $\sqrt{s} = 1.96$ TeV

V.M. Abazov,³⁶ B. Abbott,⁷⁶ M. Abolins,⁶⁶ B.S. Acharya,²⁹ M. Adams,⁵² T. Adams,⁵⁰ M. Agelou,¹⁸ J.-L. Agram,¹⁹ S.H. Ahn,³¹ M. Ahsan,⁶⁰ G.D. Alexeev,³⁶ G. Alkhazov,⁴⁰ A. Alton,⁶⁵ G. Alverson,⁶⁴ G.A. Alves,² M. Anastasoae,³⁵ T. Andeen,⁵⁴ S. Anderson,⁴⁶ B. Andrieu,¹⁷ M.S. Anzels,⁵⁴ Y. Arnoud,¹⁴ M. Arov,⁵³ A. Askew,⁵⁰ B. Åsman,⁴¹ A.C.S. Assis Jesus,³ O. Atramentov,⁵⁸ C. Autermann,²¹ C. Avila,⁸ C. Ay,²⁴ F. Badaud,¹³ A. Baden,⁶² L. Bagby,⁵³ B. Baldin,⁵¹ D.V. Bandurin,⁵⁹ P. Banerjee,²⁹ S. Banerjee,²⁹ E. Barberis,⁶⁴ P. Bargassa,⁸¹ P. Baringer,⁵⁹ C. Barnes,⁴⁴ J. Barreto,² J.F. Bartlett,⁵¹ U. Bassler,¹⁷ D. Bauer,⁴⁴ A. Bean,⁵⁹ M. Begalli,³ M. Begel,⁷² C. Belanger-Champagne,⁵ L. Bellantoni,⁵¹ A. Bellavance,⁶⁸ J.A. Benitez,⁶⁶ S.B. Beri,²⁷ G. Bernardi,¹⁷ R. Bernhard,⁴² L. Berntzon,¹⁵ I. Bertram,⁴³ M. Besançon,¹⁸ R. Beuselinck,⁴⁴ V.A. Bezzubov,³⁹ P.C. Bhat,⁵¹ V. Bhatnagar,²⁷ M. Binder,²⁵ C. Biscarat,⁴³ K.M. Black,⁶³ I. Blackler,⁴⁴ G. Blazey,⁵³ F. Blekman,⁴⁴ S. Blessing,⁵⁰ D. Bloch,¹⁹ K. Bloom,⁶⁸ U. Blumenschein,²³ A. Boehnlein,⁵¹ O. Boeriu,⁵⁶ T.A. Bolton,⁶⁰ F. Borchering,⁵¹ G. Borissov,⁴³ K. Bos,³⁴ T. Bose,⁷⁸ A. Brandt,⁷⁹ R. Brock,⁶⁶ G. Brooijmans,⁷¹ A. Bross,⁵¹ D. Brown,⁷⁹ N.J. Buchanan,⁵⁰ D. Buchholz,⁵⁴ M. Buehler,⁸² V. Buescher,²³ S. Burdin,⁵¹ S. Burke,⁴⁶ T.H. Burnett,⁸³ E. Busato,¹⁷ C.P. Buszello,⁴⁴ J.M. Butler,⁶³ P. Calfayan,²⁵ S. Calvet,¹⁵ J. Cammin,⁷² S. Caron,³⁴ W. Carvalho,³ B.C.K. Casey,⁷⁸ N.M. Cason,⁵⁶ H. Castilla-Valdez,³³ S. Chakrabarti,²⁹ D. Chakraborty,⁵³ K.M. Chan,⁷² A. Chandra,⁴⁹ D. Chapin,⁷⁸ F. Charles,¹⁹ E. Cheu,⁴⁶ F. Chevallier,¹⁴ D.K. Cho,⁶³ S. Choi,³² B. Choudhary,²⁸ L. Christofek,⁵⁹ D. Claes,⁶⁸ B. Clément,¹⁹ C. Clément,⁴¹ Y. Coadou,⁵ M. Cooke,⁸¹ W.E. Cooper,⁵¹ D. Coppage,⁵⁹ M. Corcoran,⁸¹ M.-C. Cousinou,¹⁵ B. Cox,⁴⁵ S. Crépe-Renaudin,¹⁴ D. Cutts,⁷⁸ M. Cwiok,³⁰ H. da Motta,² A. Das,⁶³ M. Das,⁶¹ B. Davies,⁴³ G. Davies,⁴⁴ G.A. Davis,⁵⁴ K. De,⁷⁹ P. de Jong,³⁴ S.J. de Jong,³⁵ E. De La Cruz-Burelo,⁶⁵ C. De Oliveira Martins,³ J.D. Degenhardt,⁶⁵ F. Déliot,¹⁸ M. Demarteau,⁵¹ R. Demina,⁷² P. Demine,¹⁸ D. Denisov,⁵¹ S.P. Denisov,³⁹ S. Desai,⁷³ H.T. Diehl,⁵¹ M. Diesburg,⁵¹ M. Doidge,⁴³ A. Dominguez,⁶⁸ H. Dong,⁷³ L.V. Dudko,³⁸ L. Duflot,¹⁶ S.R. Dugad,²⁹ A. Duperrin,¹⁵ J. Dyer,⁶⁶ A. Dyshkant,⁵³ M. Eads,⁶⁸ D. Edmunds,⁶⁶ T. Edwards,⁴⁵ J. Ellison,⁴⁹ J. Elmsheuser,²⁵ V.D. Elvira,⁵¹ S. Eno,⁶² P. Ermolov,³⁸ J. Estrada,⁵¹ H. Evans,⁵⁵ A. Evdokimov,³⁷ V.N. Evdokimov,³⁹ S.N. Fatakia,⁶³ L. Felgioni,⁶³ A.V. Ferapontov,⁶⁰ T. Ferbel,⁷² F. Fiedler,²⁵ F. Filthaut,³⁵ W. Fisher,⁵¹ H.E. Fisk,⁵¹ I. Fleck,²³ M. Ford,⁴⁵ M. Fortner,⁵³ H. Fox,²³ S. Fu,⁵¹ S. Fuess,⁵¹ T. Gadfort,⁸³ C.F. Galea,³⁵ E. Gallas,⁵¹ E. Galyaev,⁵⁶ C. Garcia,⁷² A. Garcia-Bellido,⁸³ J. Gardner,⁵⁹ V. Gavrilov,³⁷ A. Gay,¹⁹ P. Gay,¹³ D. Gelé,¹⁹ R. Gelhaus,⁴⁹ C.E. Gerber,⁵² Y. Gershtein,⁵⁰ D. Gillberg,⁵ G. Gintner,⁷² N. Gollub,⁴¹ B. Gómez,⁸ K. Gounder,⁵¹ A. Goussiou,⁵⁶ P.D. Grannis,⁷³ H. Greenlee,⁵¹ Z.D. Greenwood,⁶¹ E.M. Gregores,⁴ G. Grenier,²⁰ Ph. Gris,¹³ J.-F. Grivaz,¹⁶ S. Grünendahl,⁵¹ M.W. Grünewald,³⁰ F. Guo,⁷³ J. Guo,⁷³ G. Gutierrez,⁵¹ P. Gutierrez,⁷⁶ A. Haas,⁷¹ N.J. Hadley,⁶² P. Haefner,²⁵ S. Hagopian,⁵⁰ J. Haley,⁶⁹ I. Hall,⁷⁶ R.E. Hall,⁴⁸ L. Han,⁷ K. Hanagaki,⁵¹ K. Harder,⁶⁰ A. Harel,⁷² R. Harrington,⁶⁴ J.M. Hauptman,⁵⁸ R. Hauser,⁶⁶ J. Hays,⁵⁴ T. Hebbeker,²¹ D. Hedin,⁵³ J.G. Hegeman,³⁴ J.M. Heinmiller,⁵² A.P. Heinson,⁴⁹ U. Heintz,⁶³ C. Hensel,⁵⁹ G. Hesketh,⁶⁴ M.D. Hildreth,⁵⁶ R. Hirosky,⁸² J.D. Hobbs,⁷³ B. Hoeneisen,¹² H. Hoeth,²⁶ M. Hohlfeld,¹⁶ S.J. Hong,³¹ R. Hooper,⁷⁸ P. Houben,³⁴ Y. Hu,⁷³ Z. Hubacek,¹⁰ V. Hynek,⁹ I. Iashvili,⁷⁰ R. Illingworth,⁵¹ A.S. Ito,⁵¹ S. Jabeen,⁶³ M. Jaffré,¹⁶ S. Jain,⁷⁶ K. Jakobs,²³ C. Jarvis,⁶² A. Jenkins,⁴⁴ R. Jesik,⁴⁴ K. Johns,⁴⁶ C. Johnson,⁷¹ M. Johnson,⁵¹ A. Jonckheere,⁵¹ P. Jonsson,⁴⁴ A. Juste,⁵¹ D. Käfer,²¹ S. Kahn,⁷⁴ E. Kajfasz,¹⁵ A.M. Kalinin,³⁶ J.M. Kalk,⁶¹ J.R. Kalk,⁶⁶ S. Kappler,²¹ D. Karmanov,³⁸ J. Kasper,⁶³ P. Kasper,⁵¹ I. Katsanos,⁷¹ D. Kau,⁵⁰ R. Kaur,²⁷ R. Kehoe,⁸⁰ S. Kermiche,¹⁵ S. Kesisoglou,⁷⁸ N. Khalatyan,⁶³ A. Khanov,⁷⁷ A. Kharchilava,⁷⁰ Y.M. Kharzheev,³⁶ D. Khatidze,⁷¹ H. Kim,⁷⁹ T.J. Kim,³¹ M.H. Kirby,³⁵ B. Klima,⁵¹ J.M. Kohli,²⁷ J.-P. Konrath,²³ M. Kopal,⁷⁶ V.M. Korabely,³⁹ J. Kotcher,⁷⁴ B. Kothari,⁷¹ A. Koubarovsky,³⁸ A.V. Kozelov,³⁹ J. Kozminski,⁶⁶ A. Kryemadhi,⁸² S. Krzywdzinski,⁵¹ T. Kuhl,²⁴ A. Kumar,⁷⁰ S. Kunori,⁶² A. Kupco,¹¹ T. Kurča,^{20,*} J. Kvita,⁹ S. Lager,⁴¹ S. Lammers,⁷¹ G. Landsberg,⁷⁸ J. Lazoflores,⁵⁰ A.-C. Le Bihan,¹⁹ P. Lebrun,²⁰ W.M. Lee,⁵³ A. Leflat,³⁸ F. Lehner,⁴² V. Lesne,¹³ J. Leveque,⁴⁶ P. Lewis,⁴⁴ J. Li,⁷⁹ Q.Z. Li,⁵¹ J.G.R. Lima,⁵³ D. Lincoln,⁵¹ J. Linnemann,⁶⁶ V.V. Lipaev,³⁹ R. Lipton,⁵¹ Z. Liu,⁵ L. Lobo,⁴⁴ A. Lobodenko,⁴⁰ M. Lokajicek,¹¹ A. Lounis,¹⁹ P. Love,⁴³ H.J. Lubatti,⁸³ M. Lynker,⁵⁶ A.L. Lyon,⁵¹ A.K.A. Maciel,² R.J. Madaras,⁴⁷ P. Mättig,²⁶ C. Magass,²¹ A. Magerkurth,⁶⁵ A.-M. Magnan,¹⁴ N. Makovec,¹⁶ P.K. Mal,⁵⁶ H.B. Malbouisson,³ S. Malik,⁶⁸ V.L. Malyshev,³⁶ H.S. Mao,⁶ Y. Maravin,⁶⁰ M. Martens,⁵¹ S.E.K. Mattingly,⁷⁸ R. McCarthy,⁷³ R. McCroskey,⁴⁶ D. Meder,²⁴ A. Melnitchouk,⁶⁷ A. Mendes,¹⁵ L. Mendoza,⁸ M. Merkin,³⁸ K.W. Merritt,⁵¹ A. Meyer,²¹ J. Meyer,²²

M. Michaut,¹⁸ H. Miettinen,⁸¹ T. Millet,²⁰ J. Mitrevski,⁷¹ J. Molina,³ N.K. Mondal,²⁹ J. Monk,⁴⁵ R.W. Moore,⁵ T. Moulik,⁵⁹ G.S. Muanza,¹⁶ M. Mulders,⁵¹ M. Mulhearn,⁷¹ L. Mundim,³ Y.D. Mutaf,⁷³ E. Nagy,¹⁵ M. Naimuddin,²⁸ M. Narain,⁶³ N.A. Naumann,³⁵ H.A. Neal,⁶⁵ J.P. Negret,⁸ S. Nelson,⁵⁰ P. Neustroev,⁴⁰ C. Noeding,²³ A. Nomerotski,⁵¹ S.F. Novaes,⁴ T. Nunnemann,²⁵ V. O'Dell,⁵¹ D.C. O'Neil,⁵ G. Obrant,⁴⁰ V. Oguri,³ N. Oliveira,³ N. Oshima,⁵¹ R. Otec,¹⁰ G.J. Otero y Garzón,⁵² M. Owen,⁴⁵ P. Padley,⁸¹ N. Parashar,⁵⁷ S.-J. Park,⁷² S.K. Park,³¹ J. Parsons,⁷¹ R. Partridge,⁷⁸ N. Parua,⁷³ A. Patwa,⁷⁴ G. Pawloski,⁸¹ P.M. Perea,⁴⁹ E. Perez,¹⁸ K. Peters,⁴⁵ P. Pétroff,¹⁶ M. Petteni,⁴⁴ R. Piegai,¹ M.-A. Pleier,²² P.L.M. Podesta-Lerma,³³ V.M. Podstavkov,⁵¹ Y. Pogorelov,⁵⁶ M.-E. Pol,² A. Pompoš,⁷⁶ B.G. Pope,⁶⁶ A.V. Popov,³⁹ W.L. Prado da Silva,³ H.B. Prosper,⁵⁰ S. Protopopescu,⁷⁴ J. Qian,⁶⁵ A. Quadt,²² B. Quinn,⁶⁷ K.J. Rani,²⁹ K. Ranjan,²⁸ P.A. Rapidis,⁵¹ P.N. Ratoff,⁴³ P. Renkel,⁸⁰ S. Reucroft,⁶⁴ M. Rijssenbeek,⁷³ I. Ripp-Baudot,¹⁹ F. Rizatdinova,⁷⁷ S. Robinson,⁴⁴ R.F. Rodrigues,³ C. Royon,¹⁸ P. Rubinov,⁵¹ R. Ruchti,⁵⁶ V.I. Rud,³⁸ G. Sajot,¹⁴ A. Sánchez-Hernández,³³ M.P. Sanders,⁶² A. Santoro,³ G. Savage,⁵¹ L. Sawyer,⁶¹ T. Scanlon,⁴⁴ D. Schaile,²⁵ R.D. Schamberger,⁷³ Y. Scheglov,⁴⁰ H. Schellman,⁵⁴ P. Schieferdecker,²⁵ C. Schmitt,²⁶ C. Schwanenberger,⁴⁵ A. Schwartzman,⁶⁹ R. Schwienhorst,⁶⁶ S. Sengupta,⁵⁰ H. Severini,⁷⁶ E. Shabalina,⁵² M. Shamim,⁶⁰ V. Shary,¹⁸ A.A. Shchukin,³⁹ W.D. Shephard,⁵⁶ R.K. Shivpuri,²⁸ D. Shpakov,⁶⁴ V. Siccaldi,¹⁹ R.A. Sidwell,⁶⁰ V. Simak,¹⁰ V. Sirotenko,⁵¹ P. Skubic,⁷⁶ P. Slattery,⁷² R.P. Smith,⁵¹ G.R. Snow,⁶⁸ J. Snow,⁷⁵ S. Snyder,⁷⁴ S. Söldner-Rembold,⁴⁵ X. Song,⁵³ L. Sonnenschein,¹⁷ A. Sopczak,⁴³ M. Sosebee,⁷⁹ K. Soustruznik,⁹ M. Souza,² B. Spurlock,⁷⁹ J. Stark,¹⁴ J. Steele,⁶¹ K. Stevenson,⁵⁵ V. Stolin,³⁷ A. Stone,⁵² D.A. Stoyanova,³⁹ J. Strandberg,⁴¹ M.A. Strang,⁷⁰ M. Strauss,⁷⁶ R. Ströhmer,²⁵ D. Strom,⁵⁴ M. Strovink,⁴⁷ L. Stutte,⁵¹ S. Sumowidagdo,⁵⁰ A. Sznajder,³ M. Talby,¹⁵ P. Tamburello,⁴⁶ W. Taylor,⁵ P. Telford,⁴⁵ J. Temple,⁴⁶ B. Tiller,²⁵ M. Titov,²³ V.V. Tokmenin,³⁶ M. Tomoto,⁵¹ T. Toole,⁶² I. Torchiani,²³ S. Towers,⁴³ T. Trefzger,²⁴ S. Trincas-Duvoid,¹⁷ D. Tsybychev,⁷³ B. Tuchming,¹⁸ C. Tully,⁶⁹ A.S. Turcot,⁴⁵ P.M. Tuts,⁷¹ R. Unalan,⁶⁶ L. Uvarov,⁴⁰ S. Uvarov,⁴⁰ S. Uzunyan,⁵³ B. Vachon,⁵ P.J. van den Berg,³⁴ R. Van Kooten,⁵⁵ W.M. van Leeuwen,³⁴ N. Varelas,⁵² E.W. Varnes,⁴⁶ A. Vartapetian,⁷⁹ I.A. Vasilyev,³⁹ M. Vaupel,²⁶ P. Verdier,²⁰ L.S. Vertogradov,³⁶ M. Verzocchi,⁵¹ F. Villeneuve-Seguié,⁴⁴ P. Vint,⁴⁴ J.-R. Vlimant,¹⁷ E. Von Toerne,⁶⁰ M. Voutilainen,^{68,†} M. Vreeswijk,³⁴ H.D. Wahl,⁵⁰ L. Wang,⁶² J. Warchol,⁵⁶ G. Watts,⁸³ M. Wayne,⁵⁶ M. Weber,⁵¹ H. Weerts,⁶⁶ N. Wermes,²² M. Wetstein,⁶² A. White,⁷⁹ D. Wicke,²⁶ G.W. Wilson,⁵⁹ S.J. Wimpenny,⁴⁹ M. Wobisch,⁵¹ J. Womersley,⁵¹ D.R. Wood,⁶⁴ T.R. Wyatt,⁴⁵ Y. Xie,⁷⁸ N. Xuan,⁵⁶ S. Yacoob,⁵⁴ R. Yamada,⁵¹ M. Yan,⁶² T. Yasuda,⁵¹ Y.A. Yatsunenko,³⁶ K. Yip,⁷⁴ H.D. Yoo,⁷⁸ S.W. Youn,⁵⁴ C. Yu,¹⁴ J. Yu,⁷⁹ A. Yurkewicz,⁷³ A. Zatserklyaniy,⁵³ C. Zeitnitz,²⁶ D. Zhang,⁵¹ T. Zhao,⁸³ Z. Zhao,⁶⁵ B. Zhou,⁶⁵ J. Zhu,⁷³ M. Zielinski,⁷² D. Zieminska,⁵⁵ A. Zieminski,⁵⁵ V. Zutshi,⁵³ and E.G. Zverev³⁸

(DØ Collaboration)

¹ Universidad de Buenos Aires, Buenos Aires, Argentina

² LAFEX, Centro Brasileiro de Pesquisas Físicas, Rio de Janeiro, Brazil

³ Universidade do Estado do Rio de Janeiro, Rio de Janeiro, Brazil

⁴ Instituto de Física Teórica, Universidade Estadual Paulista, São Paulo, Brazil

⁵ University of Alberta, Edmonton, Alberta, Canada, Simon Fraser University, Burnaby, British Columbia, Canada, York University, Toronto, Ontario, Canada, and McGill University, Montreal, Quebec, Canada

⁶ Institute of High Energy Physics, Beijing, People's Republic of China

⁷ University of Science and Technology of China, Hefei, People's Republic of China

⁸ Universidad de los Andes, Bogotá, Colombia

⁹ Center for Particle Physics, Charles University, Prague, Czech Republic

¹⁰ Czech Technical University, Prague, Czech Republic

¹¹ Center for Particle Physics, Institute of Physics, Academy of Sciences of the Czech Republic, Prague, Czech Republic

¹² Universidad San Francisco de Quito, Quito, Ecuador

¹³ Laboratoire de Physique Corpusculaire, IN2P3-CNRS, Université Blaise Pascal, Clermont-Ferrand, France

¹⁴ Laboratoire de Physique Subatomique et de Cosmologie, IN2P3-CNRS, Université de Grenoble 1, Grenoble, France

¹⁵ CPPM, IN2P3-CNRS, Université de la Méditerranée, Marseille, France

¹⁶ IN2P3-CNRS, Laboratoire de l'Accélérateur Linéaire, Orsay, France

¹⁷ LPNHE, IN2P3-CNRS, Universités Paris VI and VII, Paris, France

¹⁸ DAPNIA/Service de Physique des Particules, CEA, Saclay, France

¹⁹ IReS, IN2P3-CNRS, Université Louis Pasteur, Strasbourg, France, and Université de Haute Alsace, Mulhouse, France

²⁰ Institut de Physique Nucléaire de Lyon, IN2P3-CNRS, Université Claude Bernard, Villeurbanne, France

²¹ III. Physikalisches Institut A, RWTH Aachen, Aachen, Germany

²² Physikalisches Institut, Universität Bonn, Bonn, Germany

²³ Physikalisches Institut, Universität Freiburg, Freiburg, Germany

²⁴ Institut für Physik, Universität Mainz, Mainz, Germany

²⁵ Ludwig-Maximilians-Universität München, München, Germany

- ²⁶ *Fachbereich Physik, University of Wuppertal, Wuppertal, Germany*
- ²⁷ *Panjab University, Chandigarh, India*
- ²⁸ *Delhi University, Delhi, India*
- ²⁹ *Tata Institute of Fundamental Research, Mumbai, India*
- ³⁰ *University College Dublin, Dublin, Ireland*
- ³¹ *Korea Detector Laboratory, Korea University, Seoul, Korea*
- ³² *SungKyunKwan University, Suwon, Korea*
- ³³ *CINVESTAV, Mexico City, Mexico*
- ³⁴ *FOM-Institute NIKHEF and University of Amsterdam/NIKHEF, Amsterdam, The Netherlands*
- ³⁵ *Radboud University Nijmegen/NIKHEF, Nijmegen, The Netherlands*
- ³⁶ *Joint Institute for Nuclear Research, Dubna, Russia*
- ³⁷ *Institute for Theoretical and Experimental Physics, Moscow, Russia*
- ³⁸ *Moscow State University, Moscow, Russia*
- ³⁹ *Institute for High Energy Physics, Protvino, Russia*
- ⁴⁰ *Petersburg Nuclear Physics Institute, St. Petersburg, Russia*
- ⁴¹ *Lund University, Lund, Sweden, Royal Institute of Technology and Stockholm University, Stockholm, Sweden, and Uppsala University, Uppsala, Sweden*
- ⁴² *Physik Institut der Universität Zürich, Zürich, Switzerland*
- ⁴³ *Lancaster University, Lancaster, United Kingdom*
- ⁴⁴ *Imperial College, London, United Kingdom*
- ⁴⁵ *University of Manchester, Manchester, United Kingdom*
- ⁴⁶ *University of Arizona, Tucson, Arizona 85721, USA*
- ⁴⁷ *Lawrence Berkeley National Laboratory and University of California, Berkeley, California 94720, USA*
- ⁴⁸ *California State University, Fresno, California 93740, USA*
- ⁴⁹ *University of California, Riverside, California 92521, USA*
- ⁵⁰ *Florida State University, Tallahassee, Florida 32306, USA*
- ⁵¹ *Fermi National Accelerator Laboratory, Batavia, Illinois 60510, USA*
- ⁵² *University of Illinois at Chicago, Chicago, Illinois 60607, USA*
- ⁵³ *Northern Illinois University, DeKalb, Illinois 60115, USA*
- ⁵⁴ *Northwestern University, Evanston, Illinois 60208, USA*
- ⁵⁵ *Indiana University, Bloomington, Indiana 47405, USA*
- ⁵⁶ *University of Notre Dame, Notre Dame, Indiana 46556, USA*
- ⁵⁷ *Purdue University Calumet, Hammond, Indiana 46323, USA*
- ⁵⁸ *Iowa State University, Ames, Iowa 50011, USA*
- ⁵⁹ *University of Kansas, Lawrence, Kansas 66045, USA*
- ⁶⁰ *Kansas State University, Manhattan, Kansas 66506, USA*
- ⁶¹ *Louisiana Tech University, Ruston, Louisiana 71272, USA*
- ⁶² *University of Maryland, College Park, Maryland 20742, USA*
- ⁶³ *Boston University, Boston, Massachusetts 02215, USA*
- ⁶⁴ *Northeastern University, Boston, Massachusetts 02115, USA*
- ⁶⁵ *University of Michigan, Ann Arbor, Michigan 48109, USA*
- ⁶⁶ *Michigan State University, East Lansing, Michigan 48824, USA*
- ⁶⁷ *University of Mississippi, University, Mississippi 38677, USA*
- ⁶⁸ *University of Nebraska, Lincoln, Nebraska 68588, USA*
- ⁶⁹ *Princeton University, Princeton, New Jersey 08544, USA*
- ⁷⁰ *State University of New York, Buffalo, New York 14260, USA*
- ⁷¹ *Columbia University, New York, New York 10027, USA*
- ⁷² *University of Rochester, Rochester, New York 14627, USA*
- ⁷³ *State University of New York, Stony Brook, New York 11794, USA*
- ⁷⁴ *Brookhaven National Laboratory, Upton, New York 11973, USA*
- ⁷⁵ *Langston University, Langston, Oklahoma 73050, USA*
- ⁷⁶ *University of Oklahoma, Norman, Oklahoma 73019, USA*
- ⁷⁷ *Oklahoma State University, Stillwater, Oklahoma 74078, USA*
- ⁷⁸ *Brown University, Providence, Rhode Island 02912, USA*
- ⁷⁹ *University of Texas, Arlington, Texas 76019, USA*
- ⁸⁰ *Southern Methodist University, Dallas, Texas 75275, USA*
- ⁸¹ *Rice University, Houston, Texas 77005, USA*
- ⁸² *University of Virginia, Charlottesville, Virginia 22901, USA*
- ⁸³ *University of Washington, Seattle, Washington 98195, USA*

(Dated: May 2, 2006)

A search for the production of neutral Higgs bosons Φ decaying into $\tau^+\tau^-$ final states in $p\bar{p}$ collisions at a center-of-mass energy of 1.96 TeV is presented. The data, corresponding to an

integrated luminosity of up to 348 pb^{-1} , were collected by the $D\bar{O}$ experiment at the Fermilab Tevatron Collider. Since no excess compared to the expectation from standard model processes is found, limits on the production cross section times branching ratio are set. The results are combined with those obtained from the $D\bar{O}$ search for $\Phi b(\bar{b}) \rightarrow b\bar{b}b(\bar{b})$ and are interpreted in the minimal supersymmetric standard model.

PACS numbers: 14.80.Bn, 14.80.Cp, 14.60.Fg, 13.85.Rm, 12.60.Fr, 12.60.Jv

Final states leading to high-mass tau lepton pairs can arise from various physics processes beyond the standard model including the production of neutral Higgs bosons (generally denoted as Φ). This is of particular interest in models with more than one Higgs doublet, where production rates for $p\bar{p} \rightarrow \Phi \rightarrow \tau\tau$ can potentially be large enough for an observation at the Fermilab Tevatron Collider. For instance, the minimal supersymmetric standard model (MSSM) [1] contains two complex Higgs doublets, leading to two neutral CP-even (h, H), one CP-odd (A), and a pair of charged (H^\pm) Higgs bosons. At tree level, the Higgs sector of the MSSM is fully specified by two parameters, generally chosen to be M_A , the mass of the CP-odd Higgs boson, and $\tan\beta$, the ratio of the vacuum expectation values of the two Higgs doublets. At large $\tan\beta$, the coupling of the neutral Higgs bosons to down-type quarks and charged leptons is strongly enhanced, leading to sizeable cross sections.

Searches for neutral MSSM Higgs bosons have been conducted at LEP [2] and at the Tevatron [3, 4]. In this Letter a search for $\Phi \rightarrow \tau\tau$ decays is presented. At least one of the tau leptons is required to decay leptonically, leading to final states containing $e\tau_h$, $\mu\tau_h$ and $e\mu$, where τ_h represents a hadronically decaying tau lepton.

The data were collected at the Fermilab Tevatron Collider between September 2002 and August 2004 at $\sqrt{s} = 1.96 \text{ TeV}$ and correspond to integrated luminosities of 328 pb^{-1} , 299 pb^{-1} , and 348 pb^{-1} for the $e\tau_h$, $\mu\tau_h$ and $e\mu$ final states, respectively. Final states with two electrons or two muons have a small signal-to-background ratio due to the small branching fraction and the large background from Z/γ^* production, and are therefore not considered.

A thorough description of the $D\bar{O}$ detector can be found in Ref. [5]. Briefly, the detector consists of a magnetic central tracking system surrounded by a liquid-argon and uranium calorimeter and a toroidal muon spectrometer. The central tracking system comprises a silicon microstrip tracker (SMT) and a central fiber tracker (CFT), both located within a 2 T magnetic field provided by a superconducting solenoidal magnet. The SMT and CFT designs were optimized to provide precise tracking and vertexing capabilities over the pseudorapidity range $|\eta| < 2.5$, where $\eta = -\ln(\tan(\theta/2))$ and θ is the polar angle with respect to the proton beam. The calorimeter is divided into a central section (CC) covering $|\eta| \lesssim 1.1$, and two end calorimeters (EC) that extend coverage to $|\eta| \approx 4.2$, all housed in separate cryostats. Scintillators

between the CC and EC cryostats provide sampling of developing showers for $1.1 < |\eta| < 1.4$. A muon system, at $|\eta| < 2$, consists of a layer of tracking detectors and scintillation trigger counters in front of 1.8 T toroids, followed by two similar layers after the toroids. The luminosity is measured using plastic scintillator arrays located in front of the EC cryostats, covering $2.7 < |\eta| < 4.4$.

The $e\tau_h$ and the $\mu\tau_h$ analyses rely on single electron and single muon triggers, respectively, while the $e\mu$ analysis uses dilepton triggers. The triggers exploit the typical signatures of leptons in the detector, including high-momentum tracks in the tracking system, energy deposits in the calorimeter, and hits in the muon detector.

Signal and standard model processes are modeled using the PYTHIA 6.202 [6] Monte Carlo (MC) generator, followed by a GEANT-based [7] simulation of the $D\bar{O}$ detector geometry. MC events are then reconstructed with the same programs as used for data. All background processes, apart from QCD multijet production, are normalized using cross sections calculated at next-to-leading order (NLO) and next-to-NLO (for Z boson, W boson, and Drell-Yan production) based on the CTEQ5 [8] parton distribution functions (PDF).

The normalization and shape of background contributions from QCD multijet production, where jets are misidentified as leptons, are estimated from the data themselves by using like-sign e and τ_h candidate events (in the $e\tau_h$ analysis) or by selecting background samples by inverting lepton identification criteria (in the $\mu\tau_h$ and $e\mu$ analyses). These samples are normalized to the data at an early stage of the selection in a region of phase space dominated by multijet production.

Isolated electrons are reconstructed based on their characteristic energy deposition in the calorimeter, including the transverse and longitudinal shower profile. In addition, a track must point to the energy deposition in the calorimeter, and the track momentum and calorimeter energy must be consistent. Further rejection against background from photons and jets is achieved by using a likelihood discriminant, which is exploiting characteristic calorimeter and tracking information. Muons are selected using tracks in the central tracking detector in combination with patterns of hits in the muon detector. Muons are required to be isolated in both the calorimeter and the tracker. Reconstruction efficiencies for both leptons are measured using data.

A hadronically decaying tau lepton is characterized by a narrow isolated jet with low track multiplicity. The

tau reconstruction is either seeded by calorimeter energy clusters or tracks [9]. Three τ -types are distinguished:

- τ -type 1: a single track with energy deposition in the hadronic calorimeter (1-prong, π^\pm -like);
- τ -type 2: a single track with energy deposition in the hadronic and the electromagnetic calorimeter (1-prong, ρ^\pm -like);
- τ -type 3: two or three tracks with an invariant mass below 1.1 or 1.7 GeV, respectively (3-prong).

A set of neural networks, one for each τ -type, has been developed based on further discriminating variables. The neural networks were used elsewhere for a cross section measurement of the process $Z/\gamma^* \rightarrow \tau\tau$ [9]. The input variables exploit the differences between hadronically decaying tau leptons and jets in the longitudinal and transverse shower shape as well as differences in the isolation in the calorimeter and the tracker. The training of the neural networks is performed using multijet events from data as the background sample and tau MC events as signal, resulting in a network output close to one for tau candidates and close to zero for background. For τ -types 1 and 2, hadronic tau candidates are required to have a neural network output greater than 0.9. Due to the larger background contamination, this cut value is tightened to 0.95 for τ -type 3.

Electrons and muons can be misidentified as one-prong hadronic tau decays. Hadronically decaying tau leptons deposit a significant fraction of their energy in the hadronic part of the calorimeter. To reject electrons, the ratio between the transverse energy in the hadronic calorimeter and the transverse momentum of the tau track is required to be larger than 0.4. With a smaller rate, background from muons occurs in τ -types 1 and 2 in the $\mu\tau_h$ analysis. This background is suppressed by rejecting tau candidates to which a muon can be matched.

The signal is characterized by two leptons, missing transverse momentum, and little jet activity. It would stand out as an enhancement above the background from standard model processes in the visible mass

$$M_{\text{vis}} = \sqrt{(P_{\tau_1} + P_{\tau_2} + \cancel{P}_T)^2}, \quad (1)$$

calculated using the four vectors of the visible tau decay products $P_{\tau_{1,2}}$ and of the missing momentum $\cancel{P}_T = (\cancel{E}_T, \cancel{E}_x, \cancel{E}_y, 0)$. For the optimization of the signal selection, only the high mass region is used, which is defined as $M_{\text{vis}} > 120$ GeV in the $e\tau_h$ and $\mu\tau_h$ analyses and as $M_{\text{vis}} > 110$ GeV in the $e\mu$ analysis.

In the $e\tau_h$ and $\mu\tau_h$ analyses, an isolated lepton (e, μ) and an isolated hadronic tau with transverse momenta above 14 GeV and 20 GeV respectively are required. In addition to the irreducible background from $Z/\gamma^* \rightarrow \tau\tau$ production, a $W \rightarrow \ell\nu$ decay can be misidentified as a high-mass di-tau event if it is produced in association

TABLE I: Numbers of events observed in data and expected for background and the efficiency for a signal with $M_\phi = 150$ GeV for the three analysis channels, with statistical and systematic uncertainties added in quadrature.

Analysis	$e\tau_h$	$\mu\tau_h$	$e\mu$
Data	484	575	41
QCD	199 ± 26	62 ± 7	2.1 ± 0.4
$Z/\gamma^* \rightarrow \tau\tau$	203 ± 26	492 ± 53	39 ± 5
$Z/\gamma^* \rightarrow ee, \mu\mu$	10 ± 1	5 ± 1	0.6 ± 0.1
$W \rightarrow e\nu, \mu\nu, \tau\nu$	14 ± 2	14 ± 2	0.3 ± 0.2
Di-boson	0.5 ± 0.1	3.1 ± 0.3	1.0 ± 0.1
$t\bar{t}$	0.4 ± 0.1	1.2 ± 0.2	0.06 ± 0.02
Total expected	427 ± 55	576 ± 62	44 ± 5
Efficiency %	4.8 ± 0.4	8.6 ± 0.8	4.3 ± 0.5

with an energetic jet that is misidentified as a hadronic tau decay. In these events, a strongly boosted W boson recoils against the jet, and the mass of the W boson can be reconstructed in the following approximation

$$M_W^{e/\mu} = \sqrt{2 E^\nu E^{e/\mu} (1 - \cos \Delta\phi)}, \quad (2)$$

where the azimuthal angle $\Delta\phi$ is between the lepton and the \cancel{E}_T , and $E^\nu = \cancel{E}_T \cdot E^\ell / E_T^\ell$. To suppress the large W +jet background, $M_W^{e/\mu}$ is required to be less than 20 GeV.

In the $e\mu$ analysis, two isolated leptons with $p_T > 14$ GeV are required. The dominant background contributions after the lepton selection come from the irreducible $Z/\gamma^* \rightarrow \tau\tau$ process, followed by WW , WZ , $t\bar{t}$, $W \rightarrow \ell\nu$, and multijet events. In this analysis the multijet background is suppressed by requiring $\cancel{E}_T > 14$ GeV. Background from W +jet events can be reduced using the transverse mass $M_T^{e/\mu} = \sqrt{2 p_T^{e/\mu} \cancel{E}_T (1 - \cos \Delta\phi)}$ by requiring that either $M_T^e < 10$ GeV or $M_T^\mu < 10$ GeV. Furthermore the minimum angle between the leptons and the \cancel{E}_T vector, $\min[\Delta\phi(e, \cancel{E}_T), \Delta\phi(\mu, \cancel{E}_T)]$, has to be smaller than 0.3. Finally, a cut on the scalar sum H_T of the transverse momenta of all jets in the event, $H_T < 70$ GeV, is applied to suppress contributions from $t\bar{t}$ background.

The numbers of events observed in the data and those expected from the various standard model processes are summarized in Table I. The distribution of the visible mass as well as the contributions from various background components are shown in Fig. 1. The estimate of the expected numbers of background and signal events depends on numerous measurements that introduce a systematic uncertainty: integrated luminosity (6.5%), trigger efficiency (1%–4%), lepton identification and reconstruction efficiencies (2%–5%), jet and tau energy calibration (2%–6%), PDF uncertainty (3%–4%), and modeling of multijet background (2%–9%). All except the last one are correlated between the three final states. As

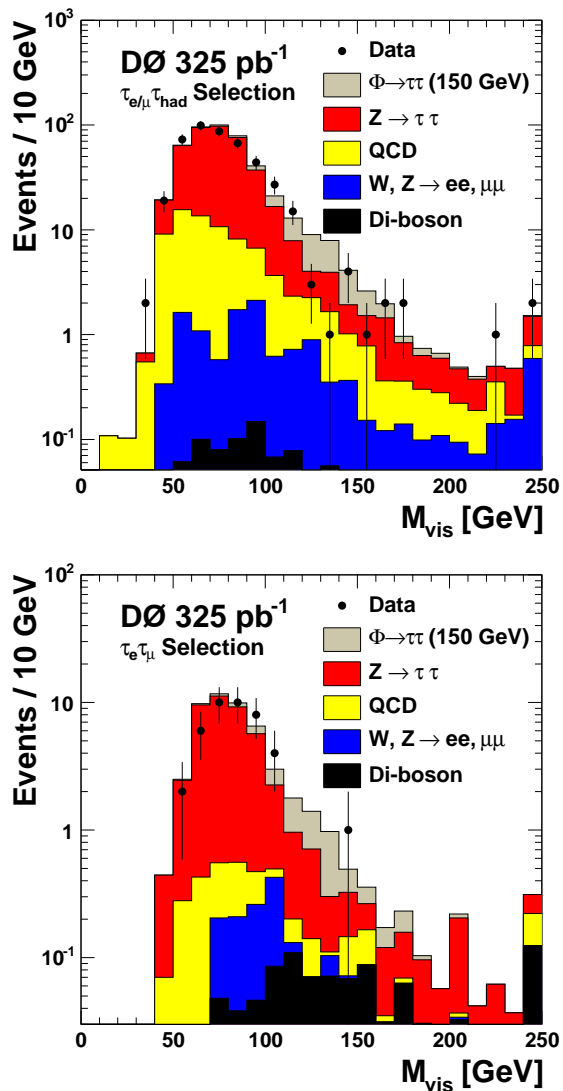


FIG. 1: The distribution of the visible mass M_{vis} for the two final states involving hadronic tau decays and for the $e\mu$ final state. The Higgs signal is normalized to the cross section excluded by this analysis. The highest bin includes the overflow, the indicated luminosity represents the average of the three final states.

can be seen from Table I and Fig. 1, good agreement is found between the numbers of events observed and those expected from standard model backgrounds.

The efficiencies for a Higgs boson signal are found to vary between 2.1%, 4.0%, and 1.2% for $M_\Phi = 100$ GeV and 9.9%, 13.6%, and 9.3% for $M_\Phi = 300$ GeV for the $e\tau_h$, $\mu\tau_h$, and $e\mu$ analyses respectively. Since no significant evidence for the production of neutral Higgs bosons with decays $\Phi \rightarrow \tau\tau$ is observed, upper limits on the production cross section times branching ratio are extracted as a function of M_Φ . In order to maximize the sensitivity (expected limit), the event samples of the $e\tau_h$

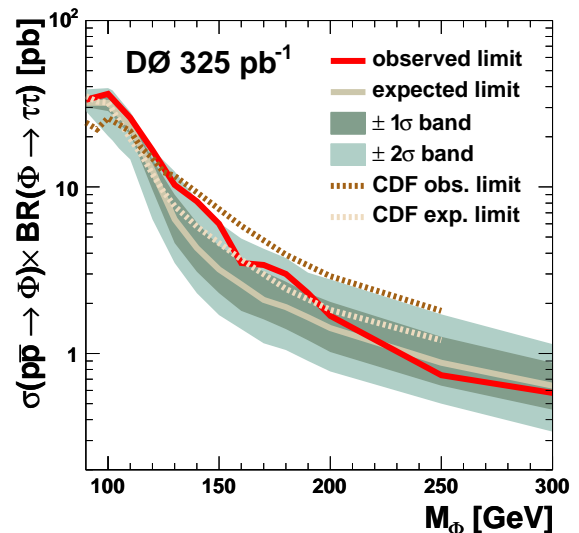


FIG. 2: The observed and expected 95% CL limits on the cross section times branching ratio for $\Phi \rightarrow \tau\tau$ production as a function of M_Φ assuming a narrow width of the Higgs boson. The error bands include systematic and statistical uncertainties. CDF curves are taken from [4], where data corresponding to an integrated luminosity of 310 pb^{-1} is used.

and $\mu\tau_h$ analyses are split into subsamples according to different signal-to-background ratios: The subsamples are separated by τ -type and by M_W ($M_W^{e,\mu} < 6$ GeV, $6 < M_W^{e,\mu} < 20$ GeV). Furthermore the differences in shape between signal and background are exploited by using the information of the full mass spectrum of M_{vis} in the limit calculation. Both the expected and the observed limits on the cross section times branching ratio at the 95% confidence level (CL), calculated using the modified frequentist approach [10], are presented in Fig. 2 as a function of M_Φ .

In the MSSM, the masses and couplings of the Higgs bosons depend, in addition to $\tan\beta$ and M_A , on the SUSY parameters through radiative corrections. In a constrained model, where unification of the SU(2) and U(1) gaugino masses is assumed, the most relevant parameters are the mixing parameter X_t , the Higgs mass parameter μ , the gaugino mass term M_2 , the gluino mass m_g , and a common scalar mass M_{SUSY} . Limits on $\tan\beta$ as a function of M_A are derived for two scenarios assuming a CP-conserving Higgs sector: the so-called m_h^{max} scenario (with the parameters $M_{\text{SUSY}} = 1$ TeV, $X_t = 2$ TeV, $M_2 = 0.2$ TeV, $\mu = \pm 0.2$ TeV, and $m_g = 0.8$ TeV) and the no-mixing scenario (with the parameters $M_{\text{SUSY}} = 2$ TeV, $X_t = 0$, $M_2 = 0.2$ TeV, $\mu = \pm 0.2$ TeV, and $m_g = 1.6$ TeV) [11]. The production cross sections, widths, and branching ratios for the Higgs bosons are calculated over the mass range from 90 to 300 GeV using the FEYNHIGGS program [12], where the

complete set of one-loop corrections and all known two-loop corrections are incorporated. The contributions of SUSY particles in the loop of the gluon fusion process are taken into account, as well as mass- and $\tan\beta$ -dependent decay widths. In the region of large $\tan\beta$, the A boson is nearly degenerate in mass with either the h or the H boson, and their production cross sections are added.

The $D\bar{O}$ results obtained in the present analysis are combined with those obtained in the $\Phi b(\bar{b}) \rightarrow b\bar{b}b(\bar{b})$ search [3], which are re-interpreted in the MSSM scenarios used in this Letter. These limits are shown in Fig. 3. For illustration purposes, the limit is shown up to $\tan\beta = 100$, ignoring the effects from potentially large higher-order corrections in the very high $\tan\beta$ regime. The combined result currently represents the most stringent limit on the production of neutral MSSM Higgs bosons at hadron colliders.

We thank S. Heinemeyer for useful discussions. We thank the staffs at Fermilab and collaborating institutions, and acknowledge support from the DOE and NSF (USA); CEA and CNRS/IN2P3 (France); FASI, Rosatom and RFBR (Russia); CAPES, CNPq, FAPERJ, FAPESP and FUNDUNESP (Brazil); DAE and DST (India); Colciencias (Colombia); CONACyT (Mexico); KRF and KOSEF (Korea); CONICET and UBACyT (Argentina); FOM (The Netherlands); PPARC (United Kingdom); MSMT (Czech Republic); CRC Program, CFI, NSERC and WestGrid Project (Canada); BMBF and DFG (Germany); SFI (Ireland); The Swedish Research Council (Sweden); Research Corporation; Alexander von Humboldt Foundation; and the Marie Curie Program.

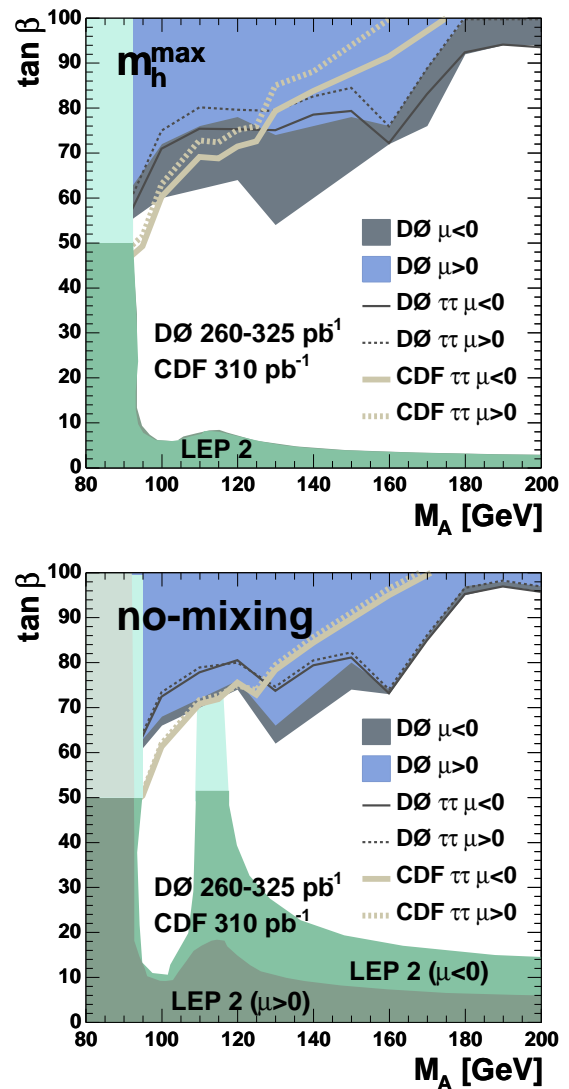


FIG. 3: Region, which is excluded at 95% CL, in the $(M_A, \tan\beta)$ plane for the m_h^{\max} and the no-mixing scenario for $\mu = +0.2$ TeV and $\mu = -0.2$ TeV ($m_{\text{top}} = 172.7$ GeV). The results obtained in the present analysis (labeled as $D\bar{O}$ $\tau\tau$) are combined with those obtained in the $\Phi b(\bar{b}) \rightarrow b\bar{b}b(\bar{b})$ search [3]. The LEP limits [2] have been extrapolated for $\tan\beta > 50$. The results of the CDF collaboration in the $\Phi \rightarrow \tau\tau$ channel [4] are also shown.

[*] On leave from IEP SAS Kosice, Slovakia.

[†] Visitor from Helsinki Institute of Physics, Helsinki, Finland.

- [1] H. P. Nilles, Phys. Rep. **110**, 1 (1984);
H. E. Haber and G. L. Kane, Phys. Rep. **117**, 75 (1985).
[2] The ALEPH, DELPHI, L3 and OPAL Collaborations, LHWG-Note 2005-01.
[3] $D\bar{O}$ Collaboration, V. Abazov *et al.*, Phys. Rev. Lett. **95**, 151801 (2005).
[4] CDF Collaboration, A. Abulencia *et al.*, Phys. Rev. Lett. **96**, 011802 (2006).
[5] $D\bar{O}$ Collaboration, V. Abazov *et al.*, physics/0507191, submitted to Nucl. Instrum. Methods in Phys. Res. A (2005).
[6] T. Sjöstrand *et al.*, Comput. Phys. Commun. **135**, 238 (2001).
[7] R. Brun and F. Carminati, CERN Program Library Long Writeup W5013 (1993).
[8] CTEQ Collaboration, H. L. Lai *et al.*, Eur. Phys. J. C

12, 375 (2000).

- [9] $D\bar{O}$ Collaboration, V. Abazov *et al.*, Phys. Rev. D **71**, 072004 (2005).
[10] T. Junk, Nucl. Instrum. Methods in Phys. Res. A **434**, 435 (1999).
[11] M. Carena, S. Heinemeyer, C. E. M. Wagner and G. Weiglein, hep-ph/0511023 (2005).
[12] S. Heinemeyer, W. Hollik and G. Weiglein, Phys. Rev. D **58**, 091701 (1998), Phys. Lett. B **440**, 296 (1998), FEYNHIGGS program: <http://www.feynhiggs.de>.